Ab Initio Calculations of Fullerenes

Gustavo E. Scuseria

Recent advances in ab initio electronic structure methods have brought about a substantial improvement in the capabilities of quantum chemists to predict and study the properties of clusters. The carbon cages known as fullerenes have been the focus of much attention because of their remarkable properties. This article discusses the application of state-of-the-art methods to representative fullerene problems and summarizes some of the recent advances and current challenges in the use of ab initio algorithms.

Since their discovery in 1985 (*1*), fullerenes—the hollow carbon cages that spontaneously self-assemble in a condensing vapor—have fascinated scientists. Fullerenes are made of an even number of three-coordinated sp^2 carbon atoms that arrange themselves into 12 pentagonal faces and any number (except 1) of hexagonal faces. The macroscopic synthesis of these nanoclusters under special conditions in a carbon arc (*2*) prompted a flurry of research that continues unabated (*3*). The most prominent representative of the fullerene class is C_{60} (buckminsterfullerene), which is the most abundant cluster in solvent-extracted carbon soot (the main source of fullerenes) and is also the smallest fullerene that satisfies the isolated pentagon rule. This rule favors the energy of structures whose pentagonal faces are separated from each other (*4*). C_{60} has a unique icosahedral structure (resembling the shape of a soccer ball) in which all atoms are symmetry-equivalent. Other fullerenes that have been produced in macroscopic quantities include C_{70}, C_{76}, C_{78}, C_{82}, C_{84}, C_{90}, and C_{96} (*5*). Fullerenes and the related carbon nanotubes (buckytubes) (*6*) have attracted the interest of chemists, physicists, and materials scientists because of their promise as superconductors (*7*), molecular containers (*8*), templates for derivatives with tailor-made electronic properties (*9*), and nanometer-wide carbon fibers (*6*). These clusters constitute a third form of elementary carbon (besides graphite and diamond) and afford a rich exohedral (outside the cage), endohedral (inside the cage), and cage-surface substitution chemistry (*10*), which makes them ideal candidates for building blocks of a carbon-based nanotechnology.

From the viewpoint of a theoretician, fullerenes are challenging molecules because of their size. The steep scaling of computational cost with molecular size prohibits quantum chemists from using their most sophisticated tools for ab initio calculations on ordinary fullerenes. The coupled cluster method, which has successfully been used to predict phenomena in small molecules (*11*), has been used for calculations on C_{20} (*12*) but not beyond. Other methods, which are less demanding in terms of computational cost but are less accurate than the coupled cluster method, have been used for much larger fullerenes: C_{60} with Moller-Plesset second-order perturbation theory (MP2) (*13*), C_{240} with density functional theory (DFT) (*14*), and C_{540} with the Hartree-Fock (HF) method (*15*). Major progress has been achieved in the last few years toward ab initio calculations on large molecular systems (*16*) with the use of HF and DFT, which are the least computationally expensive ab initio methods. The major expense in HF and DFT calculations arises from solving the electronic quantum Coulomb problem (the Coulomb repulsion between continuous charge distributions). The effective Hamiltonian diagonalization, a procedure that scales as N^3 (where N is the number of basis functions), represents only a minor portion of the computational time in calculations of molecular clusters containing up to several hundred atoms (*17*). DFT requires an additional three-dimensional numerical quadrature to obtain the exchange and correlation energies (*18*).

For many years, the basis functions of choice in ab initio quantum chemistry calculations have been Gaussians because simple analytic formulas exist for evaluating the two-electron integrals that appear in the Coulomb problem (*19*). Even when there are formally N^4 two-electron integrals to be evaluated in a molecular calculation (that is, when N is the number of basis functions, there are N^2 charge distributions, and the number of pair interactions is consequently proportional to N^4), screening techniques based on mathematical and empirical bounds can be efficiently used to identify and eliminate negligible interactions (*20*), thus reducing the scaling of the Coulomb problem to an asymptotic value of N^2 (*17*). With the use of fast multipole methods (*21–23*), much progress has recently been achieved in reducing this quadratic scaling to the near-linear regime both for energy and energy derivatives (forces) calculations (*22*).

In DFT calculations, the exchange-correlation quadrature deserves attention because its computational requirements may be steep. However, there is no fundamental limitation in achieving a linear scaling goal for this step (*24*). The accuracy of DFT methods is essentially limited by the accuracy of the exchange and correlation functionals used in the calculation, and a major effort to find better functionals is under way. Although current DFT methods are not nearly as accurate as the methods used for small molecules (*11*, *25*), DFT is the method of choice for large clusters because of its speed and scaling properties. The following examples of ab initio theoretical calculations that have contributed to our current understanding of fullerene chemistry were selected to illustrate the power and the shortcomings of these calculations.

The Smallest Fullerene: C_{20}

A dodecahedron consisting of 12 pentagons and 20 carbon atoms (Fig. 1) is topologically the smallest possible fullerene (*26*). However, in laser ablation experiments of graphite under conditions that produce fullerenes for clusters larger than C_{30}, only a monocyclic ring isomer has been found at size C_{20} (*27*). In calculations, a bowl-shaped isomer reminiscent of corannulene (Fig. 1), which minimizes the number of dangling bonds in a graphite-type structure, has been found to

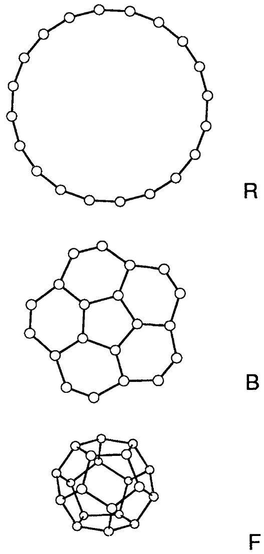

Fig. 1. The ring (R), bowl (B), and fullerene (F) isomers of C_{20}.

The author is at the Center for Nanoscale Science and Technology, Rice Quantum Institute and Department of Chemistry, Rice University, Houston, TX 77005-1892, USA.

be competitive in energy with the fullerene and ring isomers. HF calculations have predicted the ring isomer to be energetically more stable than the fullerene and bowl isomers (*28*); in contrast, calculations with both MP2 and the local density approximation (LDA) of DFT led to a reversal of the energetic ordering of the isomers (*28–30*) and predicted the fullerene to be the lowest in energy, followed by the bowl and then the ring. Calculations that used the Becke-Lee-Yang-Parr (BLYP) functional of gradient-corrected DFT reversed the ordering again (*30*) and essentially agreed with the HF results. The use of other functionals such as B3LYP (Becke three-parameter exchange with Lee-Yang-Parr correlation) and BPW91 (Becke 1988 exchange with Perdew-Wang 1991 correlation) predicted the bowl to be the most stable structure, closely followed by the fullerene (*31*). This result is consistent with both quantum Monte Carlo (*32*) and coupled cluster (*12*) predictions, although the latter favored the fullerene isomer when the energy differences were evaluated at geometries that were optimized with the HF or LDA methods.

Empirical and semiempirical predictions are of little help in predicting the most stable structure of C_{20}. The ring, bowl, and fullerene isomers contain different types as well as different numbers (20, 25, and 30, respectively) of bonds. Computed equilibrium geometries differ substantially among the methods, which only adds to the complexity of the problem. Although a definitive solution to this problem awaits further calculations, current ab initio predictions are consistent with a model in which, at high temperatures (>1500 K), entropic factors greatly favor the ring isomer over the bowl and fullerene isomers (*29, 31*). Such a model would explain the abundance of the C_{20} ring isomer in mobility experiments. The relatively low energy of the bowl isomer is consistent with an accretion ("pentagon road") mechanism of fullerene formation (*33*) in which the growing carbon sheets have enough time to anneal to their lowest energy forms, simultaneously minimizing the number of dangling bonds. The absence of the bowl isomer in mobility experiments may simply be related to entropic and kinetic (high-reactivity) factors.

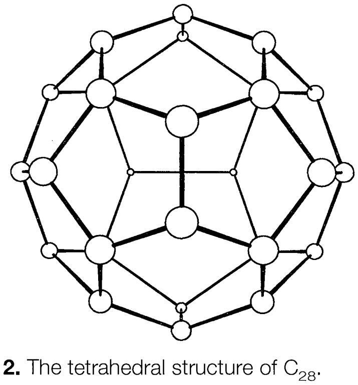

Fig. 2. The tetrahedral structure of C_{28}.

C_{28}: A Metal-Trapping Tetravalent Fullerene

The T_d structure (Fig. 2) is the most symmetrical arrangement possible for 28 identical atoms. The C_{28} cluster may best be understood as four hexagons connected by four carbon atoms at the center of triplets of fused pentagons in tetrahedral positions. Laser vaporization experiments of graphite mixtures have shown that U@C_{28} (a uranium atom trapped inside the C_{28} cage) was formed in abundance (*34*). Ab initio HF calculations have predicted that the ground state of this cluster has an open-shell electronic structure with four unpaired spins ($^5A_2$ ground state). Further calculations revealed that C_{28} should behave like a hollow superatom (with an effective valence of 4) and should be reactive toward both the inside and outside of the cage (*34, 35*). Besides uranium, metals such as scandium, titanium, zirconium, and hafnium have also been trapped inside C_{28} (*35*). Exohedral derivatives such as $C_{28}H_4$ have been predicted to be remarkably stable (*35*), although they have not yet been experimentally isolated.

Calculated binding energies of metal atoms inside small fullerenes have offered important clues about the mechanism of metal trapping and fullerene self-assembly in a condensing vapor. Theoretical predictions indicate that elements with low electronegativity have energetically favorable interactions with the fullerene cage. These elements, which form strong charge transfer complexes with graphene sheets of high electron affinity, are essentially the only elements that spontaneously form endohedral complexes. The relative absence of empty fullerenes in the same experiments implies that during the growth process, fullerene cages are to some extent nucleated around the metal atom (*35*). In contrast to the results for C_{20}, theoretical predictions at the HF (*35*), DFT (*36*), and configuration interaction levels of theory (*37*) show a consistent qualitative picture for the equilibrium geometries and electronic structures of C_{28} and its endohedral derivatives. These ab initio calculations have offered insight into the bonding properties of these clusters (*35–37*) and have also played an important role in the interpretation of the experimental data (*34*).

Annealing and Fragmentation

Under intense laser irradiation, fullerenes such as C_{60} fragment by losing C_2 units in a unique pattern that produces only even-numbered carbon clusters down to C_{32} (*38*). Close alliance between theory and experiment has been useful in elucidating the relation between fragmentation and annealing, the process by which these clusters can rearrange their surface bonding. Calculations at the HF and DFT levels of theory have produced conclusive evidence that annealing and fragmentation are high-energy reactions in which sp^3-hybridized carbons and seven-membered rings play an important role (*39*).

The Stone-Wales transformation (*40*) (Fig. 3, I) is the basic process by which fullerenes can rearrange the surface distribution of pentagons and hexagons. An alternative path, consisting of two sequential 1-2 carbon shifts (Fig. 3, II), connects the same reactants and products and has been predicted to have a lower activation energy in ab initio calculations (*39*). The interme-

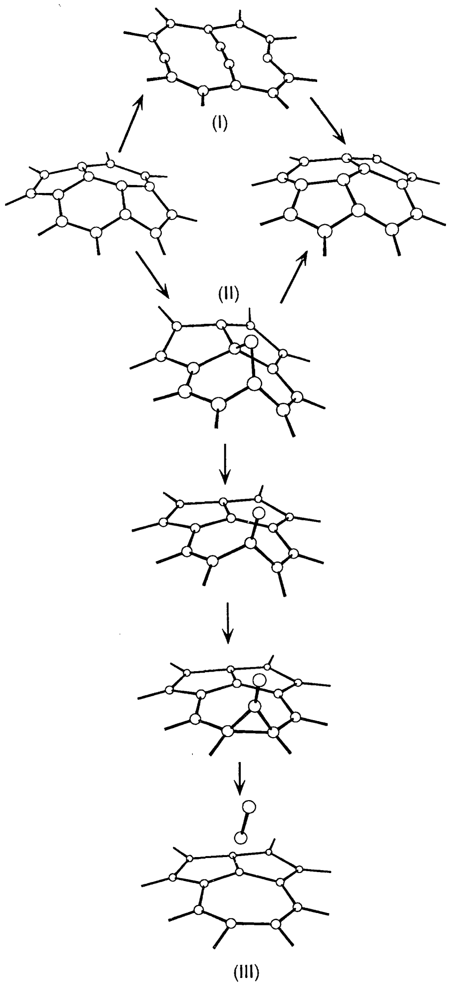

Fig. 3. The Stone-Wales rearrangement (I) is a concerted process in which two bonds form and two bonds break. An alternative path in the potential energy surface consisting of two sequential 1-2 carbon shifts has an sp^3 intermediate (II), which also connects the annealing process with C_2 fragmentation (III).

diate containing the sp^3-hybridized carbon (Fig. 3, II) is especially important because it connects the processes of annealing and fragmentation. Fragmentation proceeds from this intermediate by excision of a C_2 unit (Fig. 3, III). The amount of energy required to remove C_2 from C_{60}, however, is in dispute; experiments (*41*) and theory (*42*) predict values that differ by several electron volts.

The C_2 photofragmentation of fullerenes has an end point at C_{32}, after which shattering into small carbon species occurs. HF and DFT calculations have shown that after formation of the precursor (Fig. 4, top) for C_2 fragmentation in C_{32} (Fig. 4, left), reclosing of the cage may be impeded by the large strain, leading to a competitive fragmentation channel in the potential energy surface (Fig. 4, right), which in turn leads to excision of long carbon chains. HF and DFT calculations have also shown that this alternative fragmentation channel is energetically not competitive in C_{34} and in larger clusters that have less cage strain and can reclose more easily. These theoretical predictions (*43*) are consistent with the experimental evidence for $C_{34} \rightarrow C_{32} + C_2$ as the only fragmentation channel at this fullerene size (*38*).

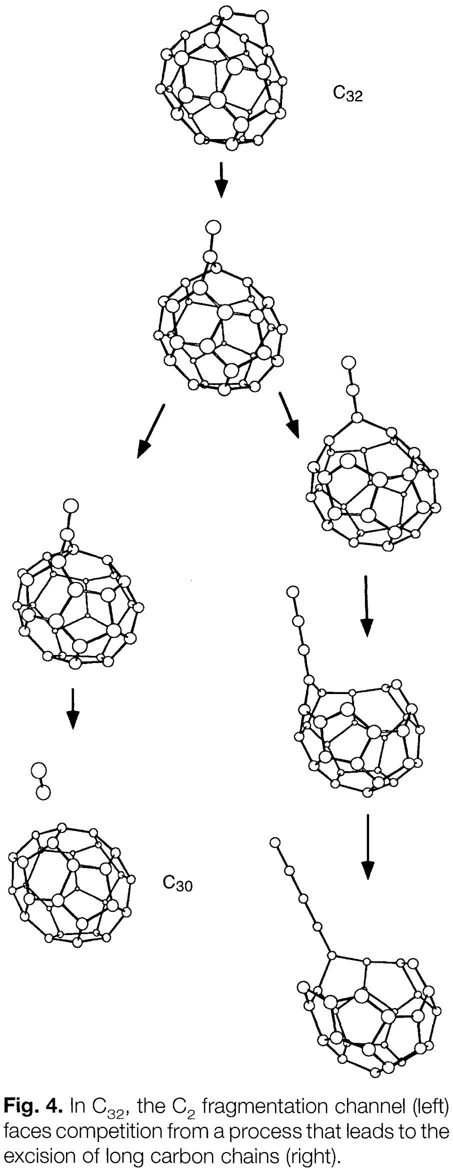

Fig. 4. In C_{32}, the C_2 fragmentation channel (left) faces competition from a process that leads to the excision of long carbon chains (right).

Giant Fullerenes: Spheres or Tubes?

The discovery of buckytubes in a deposit at the electrodes of the same machine that produces fullerenes in macroscopic quantities suggested that carbon cylinders could be competitive in energy with carbon spheroids. However, HF calculations (*44*) promptly repudiated this notion by showing that the icosahedral structure of fullerenes such as C_{180} and C_{240} was much more stable than the structures of cylindrical forms, in agreement with semiempirical predictions (*45*). Under intense electron beam irradiation, carbon soot particles and buckytubes curl into quasi-spherical particles composed of concentric graphitic shells, which clearly suggests that these "buckyonions" are more stable than any other form of carbon (including graphite) for systems of finite size (*46*). Thus, theory and experiment agree that the formation mechanism of the multishell nanotubes found at the electrodes of the arc generator must be kinetically driven.

Large yields of single-shell buckytubes were recently reported in a process identical to the laser vaporization experiment used to make fullerenes and endohedral metallofullerenes (*47*). However, the synthesis of these buckytubes occurred only in the presence of elements with large electronegativities, which do not form endohedral fullerenes, as discussed above. These results suggest that buckytubes and fullerenes may share a common growth mechanism in which distinct metal particles catalyze the formation of one class versus the other. Further calculations to determine the intermediates of metal-carbon clusters may help to elucidate the mechanism of carbon nanotube and metallofullerene growth.

Polyhedral or Spherical Shape?

The geometrical shape of the large icosahedral fullerenes C_{240} and C_{540} has been the subject of much attention. The question under investigation is whether these fullerenes possess a spherical or polyhedral (faceted) shape. This question was prompted by transmission electron microscopy (TEM) pictures that showed evidence of spheroidal shapes in concentric carbon particles (*46*, *48*). On close inspection, polyhedral outlines were discernible in some of these pictures (*48*). Simulated TEM of icosahedral fullerenes can yield images with polyhedral or spherical shapes, depending on the axis of view (*49*). Early claims that icosahedral C_{240} has multiple minima corresponding to spherical and faceted structures (*50*) have not been confirmed by ab initio calculations carried out at the HF (*14*, *15*, *44*) and DFT (*51*) levels; these calculations only showed evidence of a faceted fullerene. For icosahedral C_{540} (Fig. 5), the situation is similar: HF theory predicts the existence of only one minimum in the potential energy surface (*15*). Unlike the views along the C_2 and C_3 symmetry axes, which yield strongly faceted shapes, the view along the C_5 axis is much more spheroidal (Fig. 5), essentially in agreement with the simulated TEM images of icosahedral particles that indicated different shapes at different angles of observation. In both C_{240} and C_{540}, the predicted equilibrium structures consist of 12 pentagons that concentrate most of the strain, with fairly flat pieces of graphene sheets connecting them (*15*). The nearly spherical structure of the buckyonions observed experimentally could origi-

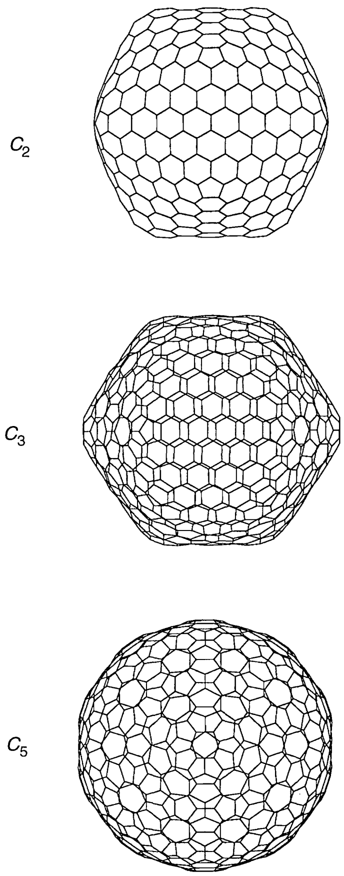

Fig. 5. Three views of the HF equilibrium structure of icosahedral C_{540} along the C_2, C_3, and C_5 symmetry axes. The C_2 and C_3 views show a faceted structure, whereas the C_5 view has a spheroidal outline because of the image superposition of the front and back carbon shells.

nate from rotational averaging (*52*) or from the presence of defects that smooth the strain at the pentagons (*53*). However, the earlier TEM images of nonannealed carbon particles (*48*) are consistent with the polyhedral shapes predicted by theory.

Conclusion

Ab initio calculations at the HF and DFT levels of theory have substantially contributed to many aspects of fullerene chemistry. For problems such as the determination of the structure of C_{20}, these two methods are not sufficiently accurate to provide reliable answers, and a higher level of theory is required. However, the speed and scaling properties of DFT make it ideal for molecular and solid-state studies (*54*) of fullerene derivatives (*55*) and buckytubes (*56*), and for future calculations on even larger clusters than those discussed above. The current challenge is to develop DFT algorithms that scale linearly with cluster size, as well as better functionals that can reproduce the results of more accurate ab initio quantum chemistry methods and experiments.

REFERENCES AND NOTES

1. H. W. Kroto, J. R. Heath, S. C. O'Brien, R. F. Curl, R. E. Smalley, *Nature* **318**, 162 (1985).
2. W. Krätschmer, L. D. Lamb, K. Fostiropoulos, D. R. Huffman, *ibid.* **347**, 354 (1990).
3. J. Cioslowski, *Electronic Structure Calculations on Fullerenes and Their Derivatives* (Oxford Univ. Press, New York, 1995).
4. H. W. Kroto, *Nature* **329**, 529 (1987); T. G. Schmalz, W. A. Seitz, D. J. Klein, G. E. Hite, *J. Am. Chem. Soc.* **110**, 1113 (1988).
5. F. Diederich *et al., Science* **252**, 548 (1991); F. Diederich *et al., ibid.* **254**, 1768 (1991); K. Kikuchi *et al., Nature* **357**, 142 (1992).
6. S. Iijima, *Nature* **354**, 56 (1991).
7. A. F. Hebard *et al., ibid.* **350**, 600 (1991).
8. M. Saunders, H. A. Jiménez-Vázquez, R. J. Cross, R. J. Poreda, *Science* **259**, 1428 (1993); R. L. Murry and G. E. Scuseria, *ibid.* **263**, 791 (1994).
9. S. H. Friedman *et al., J. Am. Chem. Soc.* **115**, 6506 (1993); J. C. Hummelen, M. Prato, F. Wudl, *ibid.* **117**, 7003 (1995).
10. R. Taylor and D. R. M. Walton, *Nature* **363**, 685 (1993).
11. T. J. Lee and G. E. Scuseria, in *Quantum Mechanical Electronic Structure Calculations with Chemical Accuracy*, S. R. Langhoff, Ed. (Kluwer, Dordrecht, Netherlands, 1995), pp. 47–108.
12. P. R. Taylor, E. Bylaska, J. H. Weare, R. Kawai, *Chem. Phys. Lett.* **235**, 558 (1995).
13. M. Häser, J. Almlöf, G. E. Scuseria, *ibid.* **181**, 497 (1991).
14. D. Bakowies, M. Bühl, W. Thiel, *ibid.* **247**, 491 (1995).
15. G. E. Scuseria, *ibid.* **243**, 193 (1995).
16. J. Almlöf, K. Faegri Jr., K. Korsell, *J. Comput. Chem.* **3**, 2469 (1986); M. J. Frisch, M. Head-Gordon, J. A. Pople, *Chem. Phys. Lett.* **166**, 275 (1990).
17. D. L. Strout and G. E. Scuseria, *J. Chem. Phys.* **102**, 8448 (1995).
18. R. G. Parr and W. Yang, *Density Functional Theory of Atoms and Molecules* (Oxford Univ. Press, New York, 1989).
19. S. F. Boys, *Proc. R. Soc. London Ser. A* **200**, 542 (1950); S. F. Boys, G. B. Cook, C. M. Reeves, I. Shavitt, *Nature* **178**, 1207 (1956).
20. M. Häser and R. Ahlrichs, *J. Comput. Chem.* **10**, 104 (1989).
21. L. Greengard, *Science* **265**, 909 (1994); C. A. White, B. G. Johnson, P. M. W. Gill, M. Head-Gordon, *Chem. Phys. Lett.* **230**, 8 (1994).
22. M. C. Strain, G. E. Scuseria, M. J. Frisch, *Science* **271**, 51 (1996); J. C. Burant, M. C. Strain, G. E. Scuseria, M. J. Frisch, *Chem. Phys. Lett.* **248**, 43 (1996).
23. M. Challacombe, E. Scwegler, J. Almlöf, in *Computational Chemistry: Review of Current Trends*, J. Leczszynski, Ed. (World Scientific, Singapore, in press).
24. R. E. Stratmann and G. E. Scuseria, in preparation.
25. C. W. Bauschlicher Jr. and S. R. Langhoff, *Science* **254**, 394 (1991).
26. P. W. Fowler and D. E. Manolopoulos, *An Atlas of Fullerenes* (Oxford Univ. Press, New York, 1995).
27. G. von Helden, N. G. Gotts, M. T. Bowers, *Nature* **363**, 60 (1993); J. Hunter, J. Fye, M. F. Jarrold, *Science* **260**, 784 (1993).
28. V. Parasuk and J. Almlöf, *Chem. Phys. Lett.* **184**, 187 (1991); M. Feyereisen, M. Guotowski, J. Simons, J. Almlöf, *J. Chem. Phys.* **96**, 2926 (1992).
29. C. J. Brabec *et al., Phys. Rev. B* **46**, 7326 (1992).
30. K. Raghavachari *et al., Chem. Phys. Lett.* **214**, 357 (1993).
31. J. M. L. Martin, J. El-Yazal, J.-P. Francois, *ibid.* **248**, 345 (1996).
32. J. C. Grossman, L. Mitas, K. Raghavachari, *Phys. Rev. Lett.* **75**, 3870 (1995).
33. R. E. Smalley, *Acc. Chem. Res.* **25**, 98 (1992).
34. T. Guo *et al., Science* **257**, 1661 (1992).
35. T. Guo, R. E. Smalley, G. E. Scuseria, *J. Chem. Phys.* **99**, 352 (1993).
36. B. I. Dunlap, O. D. Häberlen, N. Rösch, *J. Phys. Chem.* **96**, 9095 (1992); O. D. Häberlen, N. Rösch, B. I. Dunlap, *Chem. Phys. Lett.* **200**, 418 (1992).
37. D. F. Tuan and R. M. Pitzer, *J. Phys. Chem.* **99**, 9762 (1995); *ibid.*, in press; K. Zhao and R. M. Pitzer, in preparation.
38. S. C. O'Brien, J. R. Heath, R. F. Curl, R. E. Smalley, *J. Chem. Phys.* **88**, 220 (1988).
39. R. L. Murry, D. L. Strout, G. K. Odom, G. E. Scuseria, *Nature* **366**, 665 (1993); *Int. J. Mass Spectrom. Ion Processes* **138**, 113 (1994).
40. A. J. Stone and D. J. Wales, *Chem. Phys. Lett.* **128**, 501 (1986).
41. P. Sandler, C. Lifshitz, C. E. Klots, *ibid.* **200**, 445 (1992); M. Foltin, M. Lezius, P. Scheier, T. D. Märk, *J. Chem. Phys.* **98**, 9624 (1993); R. L. Whetten and C. Yeretzian, *Int. J. Mod. Phys.* **6**, 3801 (1992).
42. W. C. Eckhoff and G. E. Scuseria, *Chem. Phys. Lett.* **216**, 399 (1993); J.-Y. Yi and J. Bernholc, *J. Chem. Phys.* **96**, 8634 (1992).
43. L. P. Delabroy and G. E. Scuseria, unpublished results.
44. G. E. Scuseria, in *Buckminsterfullerenes,* W. E. Billups and M. A. Ciufolini, Eds. (VCH, New York, 1992), pp. 103–124.
45. D. Bakowies and W. Thiel, *J. Am. Chem. Soc.* **113**, 3704 (1991); G. B. Adams, O. F. Sankey, J. B. Page, M. O'Keeffe, D. A. Drabold, *Science* **256**, 1792 (1992).
46. D. Ugarte, *Nature* **359**, 707 (1992); *Carbon* **33**, 989 (1995).
47. T. Guo *et al., Chem. Phys. Lett.* **243**, 49 (1995).
48. S. Iijima, *J. Cryst. Growth* **50**, 675 (1980).
49. K. G. McKay, H. W. Kroto, D. J. Wales, *J. Chem. Soc. Faraday Trans.* **88**, 2815 (1992).
50. D. York, J. P. Lu, W. Yang, *Phys. Rev. B* **49**, 8526 (1994).
51. D. Bakowies, M. Buehl, W. Thiel, *J. Am. Chem. Soc.* **117**, 10113 (1995); B. I. Dunlap *et al., J. Phys. Chem.* **95**, 8737 (1991).
52. D. Ugarte, *Chem. Phys. Lett.* **207**, 473 (1993).
53. C. J. Brabec, A. Maiti, J. Bernholc, *ibid.* **219**, 473 (1994).
54. W. Andreoni, *J. Phys. Chem. Solids* **54**, 1789 (1993); G. E. Scuseria, in *Modern Electronic Structure Theory*, D. R. Yarkony, Ed. (World Scientific, Singapore, 1995), pp. 279–310.
55. D. L. Strout *et al., Chem. Phys. Lett.* **214**, 576 (1993); M. I. Heggie, C. D. Latham, R. Jones, P. R. Briddon, *Phys. Rev. B* **50**, 5937 (1994); A. Curioni, P. Giannozzi, J. Hutter, W. Andreoni, *J. Phys. Chem.* **99**, 4008 (1995); M. P. Pederson and A. A. Quong, *Phys. Rev. Lett.* **74**, 2319 (1995).
56. J.-C. Charlier and J.-P. Michenaud, *Phys. Rev. Lett.* **70**, 1858 (1993); J.-C. Charlier, X. Gonze, J.-P. Michenaud, *Europhys. Lett.* **29**, 43 (1995); J. W. Mintmire and C. T. White, *Carbon* **33**, 893 (1995).
57. Supported by grants from the Air Force Office of Scientific Research (F49620-95-1-0203), NSF (CHE-9321297), the Petroleum Research Fund administered by the American Chemical Society (28219-AC4), and the Welch Foundation (C-1196).